

Influence of Irradiation and Damage Coefficient on the Minority Carrier Density in Transient Response for a Bifacial Silicon Solar Cell

Idrissa GAYE, Mohamed Abderrahim Ould El Moujtaba, Ndeye THIAM, Ibrahima TALL and Grégoire SISSOKO

Laboratory of Semiconductors and Solar Energy, Physics Department, Faculty of Science and Technology, University Cheikh Anta Diop, Dakar, Senegal (gssissoko@yahoo.com)

Abstract - This paper present the theoretical and simulation investigation of a bifacial silicon solar cell under multispectral illumination and particles (electrons, protons...) irradiation. The bifacial solar cell is placed in a fast switch interrupted circuit and the transient decay is obtained between two operating point. Three cases of illumination have been considered: the front illumination, the back-side illumination and simultaneous illumination of both front and back-side. The transient variation of minority carriers' density is presented and we show how it's depending on the irradiation parameters (energy Φ and damage coefficient K_I of particles).

Keywords - 1- Bifacial, 2- Solar cell, 3- Transient variation, 4- Irradiation.

1. INTRODUCTION

Solar energy is used for satellites and other space stations. Most solar panels are made of silicon semiconductor materials, and they are subjected to effects of radiation, which are able to change the minority carrier density. There are several methods of characterization, and for this study, we use the varying operating point method. When there is an important absorption of a dose of irradiation, the electrons and holes concentration are modified and the solar cells parameters could be strongly modified. The radiation sources for semiconductors are of two sorts: natural phenomena and those from human activities.

All these phenomena generate emissions of particles and radiation which interact with matter and introduce disturbances in the atomic structures. [1]

When energetic particles go through the atomic lattice of the material, they transfer their energy to the network through events in which ionizing electrons in the network are temporarily excited to higher energy levels and events in which non-ionizing collisions between the incident particle and the target atoms causes displacement of the atoms in the lattice. It is the permanent displacement produced by non-ionizing events incident (protons and electrons) that degrades the performance of the semiconductor devices. [2]

The purpose of this study is to show the influence of the irradiation energy Φ and the damage coefficient K_I on bifacial silicon solar cell, particularly on the following

phenomenological and electrical parameters: minority carriers' density, transient photovoltage, transient photocurrent density and transient capacitance.

2. EXPERIMENTAL SETUP

The experimental setup used to obtain the transient response of the solar cell is presented by the Figure 1.

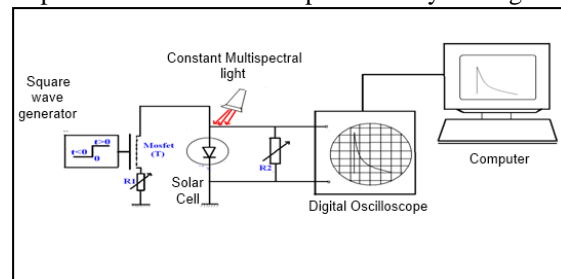


Figure 1: Experimental setup

This setup includes a square wave generator (BRI8500) which drives a RFP50N06 MOSFET type, two adjustable resistors R_1 and R_2 , a silicon solar cell, a digital oscilloscope, a computer and multi-spectral light source. The I-V curve of the solar cell is given in Figure 2. [3]-[12]-[13]

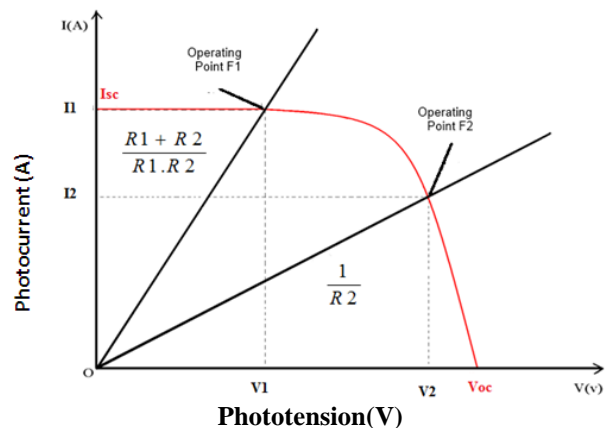


Figure 2 : I-V curve photovoltage of a silicon solar cell

- At time $t < 0$ (Figure 1), the solar cell is under constant multispectral illumination, MOSFET T is turned off and the solar cell is loaded only by resistor R_2 : this correspond to operating point F2 in steady state.
- At $t = 0$ (Figure 1), MOSFET T turning on and after a very short time (600-800ns) it is fully turned on so

that resistor R2 is in parallel with R1 + R_{dson}. R_{dson} is the drain (D) - source (S) resistance. For a sufficient Gate voltage, the value of R_{dson} is very low (less than one ohm) and can be neglected compared to that of R1 (10Ω to 4.7 kΩ). The solar cell is then at the operating point F1 in steady state (Figure 2).

The transient decay occurs between the operating points F1 and F2. The transient voltage across the solar cell is recorded by a digital oscilloscope (Tektronix), coupled with a computer for processing and analysis.

NB: Varying R1 and R2, lead to changing operating points F1 and F2 respectively; this allow us to perform the transient decay at any operating point of the bifacial solar cell.

3. THEORY

The silicon solar cell study is a n⁺pp⁺ BSF type. Given that We focus here on the base contribution of the bifacial cell and neglect the emitter. We also assume a Quasi Neutral Base (QNB) p-type, low injection condition and no lateral effect; then, the principal transport mechanism is a one-dimension diffusion of minority carriers (electrons).

Our analysis will be conducted only in this region of the solar cell. The solar cell is under constant multispectral illumination. At time t and at the depth x in the base, the distribution of the minority charge carriers is represented by n(x,t) in transient state.

We note that n(x) is the distribution of minority charge carriers in the steady state and δ(x,t) the excess minority carriers at time t from the final state, we have: [4]

$$\delta(x,t) = n(x,t) - n(x,0) \quad (1)$$

Distribution of minority carrier's n(x,t) at time t satisfies the continuity equation on the charge carriers given by:

$$D \frac{\partial^2 n(x,t)}{\partial x^2} - \frac{n(x,t)}{\tau} + G(x) = \frac{\partial n(x,t)}{\partial t} \quad (2)$$

D is the diffusion constant and L is the diffusion length of the minority carriers.

G(x) is the carrier generation rate at the depth x in the base.

$$G(x) = n \sum_{m=1}^3 a_m e^{-b_m x} \quad (3)$$

n is the illumination level, H is the thickness of the base, a_m and b_m are coefficients tabulated from overall AM1.5 solar radiation [2].

L depend on the irradiation energy Φ and the damage coefficient Kl through the following expression: [5, 2, 6]

$$L(Kl, \phi) = \frac{1}{\sqrt{\left(\frac{1}{L_0^2} + Kl \cdot \phi\right)}} \quad (4)$$

L₀ is the diffusion length without irradiation.

We present on figure 3 the diffusion length versus particles energy for various damage coefficients.

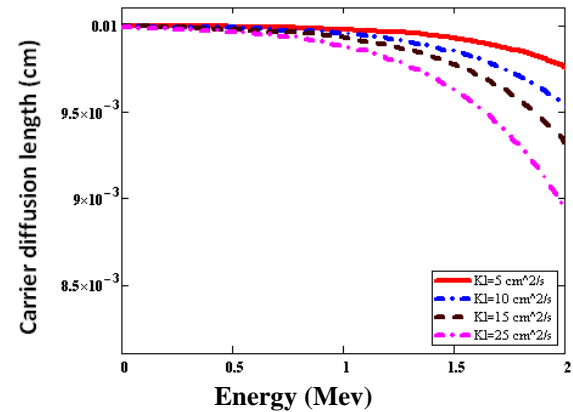


Figure 3: Profile of the variation of the diffusion length depending on the irradiation energy

The diffusion length decreases as the particle energy increases, and also with the coefficient damage, but this is more marked for higher irradiation energy (over 3 Mev). It is clear that the behaviour of the solar cell will also be influenced by irradiation.

The diffusion length is related to the lifetime of carriers by the following relationship

$$L = \sqrt{D \cdot \tau} \quad (5)$$

From this relationship, we can show the dependence of carriers lifetime with energy irradiation Φ.

This relation shows that the lifetime is sensitive to light. Even at low doses, life drops significantly, which immediately affects the performance of the solar cell. From this expression τ (5), we have the following equality

$$\frac{\tau_0}{\tau} - 1 = D \cdot \tau_0 \cdot Kl \cdot \Phi \quad (6)$$

The variation of the component $\frac{\tau_0}{\tau} - 1$ gives the value

of Kl from the slope $a = D \cdot \tau_0 \cdot Kl$

Indeed, there is a linear relationship between the ratio of lifetimes (before and after irradiation) and the irradiation energy. Figure 2.5 reflects this linearity.

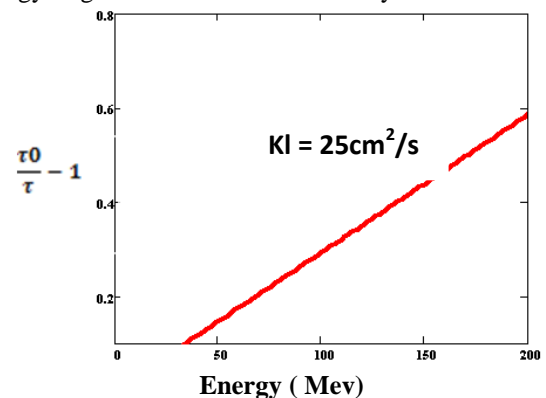


Figure 4: Profile of the variation of ratio of lifetime depending on the irradiation energy

The slope is the coefficient of damage: $K1 = 25 \text{ cm}^2 / \text{s}$
 The analysis of the variation in the ratio of lifetimes depending Φ gives the value of leading coefficient which corresponds to the coefficient of damage.

Equation (1) is solved by taking into account the boundary conditions at the junction and at the back side of the solar cell [7, 8]:

At the junction ($x = 0$):

$$D \cdot \left. \frac{\partial \delta(x)}{\partial x} \right|_{x=0} = S_f \cdot \delta(0) \quad (7)$$

At the back surface ($x = H$):

$$D \cdot \left. \frac{\partial \delta(x)}{\partial x} \right|_{x=H} = -S_b \cdot \delta(H) \quad (7) \text{ bis}$$

S_f and S_b are respectively the minority carrier's recombination velocities at the junction and at the back side of the cell.

Expressions (1), (2) and (3) represent Sturm Liouville's system.

The excess minority carrier's density can be written in the following form:

$$\delta(x, t) = \sum X_n(x) T_n(t) \quad (8)$$

The solutions of these differential equations in $X(x)$ and $T(t)$ lead to the following general terms:

$$X_n(x) = A_n \cdot \cos\left(\frac{\omega_n}{\sqrt{D}} \cdot x\right) + B_n \cdot \sin\left(\frac{\omega_n}{\sqrt{D}} \cdot x\right) \quad (9)$$

And

$$T_n(t) = T_n(0) \cdot \exp\left[-\left(\omega_n^2 + \frac{1}{\tau_{c,n}}\right) \cdot t\right] \quad (10)$$

A_n , B_n and $T_n(0)$ are constants.

$\tau_{c,n}$ is the decay time constant and is related to the minority carriers lifetime by the following expression.

$$\frac{1}{\tau_{c,n}} = \frac{1}{\tau} + \omega_n^2 \quad (11)$$

ω_n is the Eigen value of the transcendental equation below.

We can establish the following transcendental equation, taking into account the expression of L

$$\tan\left(\frac{\omega_n \cdot H \cdot \sqrt{\tau}}{L}\right) = \frac{\omega_n \cdot \sqrt{\tau} \cdot L \cdot (S_f + S_b)}{L^2 \cdot \omega_n^2 - \tau \cdot S_b \cdot S_f} \quad (12)$$

This equation is valid only if:

$$L^2 \cdot \omega_n^2 \neq \tau \cdot S_b \cdot S_f \text{ and}$$

$$\frac{\omega_n \cdot H}{D} \in \left[0, \frac{\pi}{2}\right] \cup \left[\left(n - \frac{1}{2}\right) \cdot \pi; \left(n + \frac{1}{2}\right) \cdot \pi\right] \quad (13)$$

The boxed numbers 1 and 2, which will appear in the different graphs represent the right side and the left side

of the transcendental equation. We give in tabular form corresponding to each eigenvalue solutions of the transcendental equation. The fundamental mode is $n = 0$ and if $n \neq 0$ was the harmonic of order n . The solutions of the transcendental equation (12) are given by the points of intersection of the two curves $\psi(\omega)$ and $\varphi(\omega)$. ω is the angular frequency, is expressed in $\text{rad} \cdot \text{s}^{-1}$.

The solutions of the transcendental equation (12) are given by the points of intersection of the two curves $\psi(\omega)$ and $\varphi(\omega)$. ω is the angular frequency, is expressed in $\text{rad} \cdot \text{s}^{-1}$.

$$\psi(\omega) = \tan\left(\frac{\omega_n \cdot H \cdot \sqrt{\tau}}{L}\right) \text{ et}$$

$$\varphi(\omega) = \frac{\omega_n \cdot \sqrt{\tau} \cdot L \cdot (S_f + S_b)}{L^2 \cdot \omega_n^2 - \tau \cdot S_b \cdot S_f}$$

We present on figure 5, 6, 7 a graphical resolution of the transcendental equation for illumination respectively on the front, back and simultaneous on both sides of the solar cell.

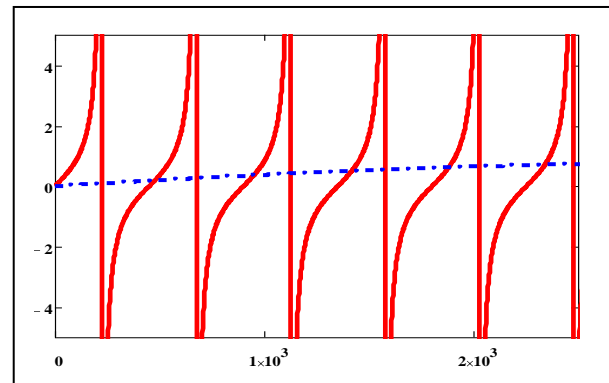


Figure 5: Graphical resolution of the transcendental equation for the front illumination

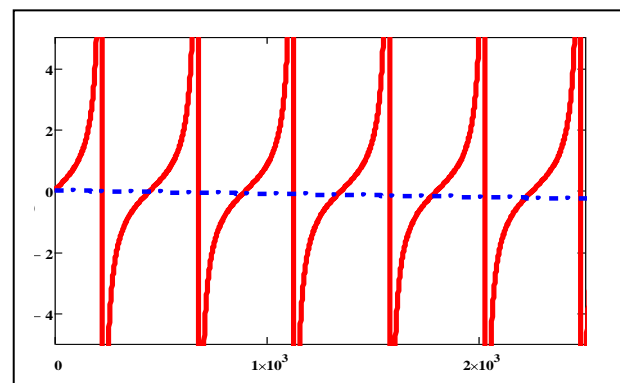


Figure 6: Graphical resolution of the transcendental equation for the back illumination

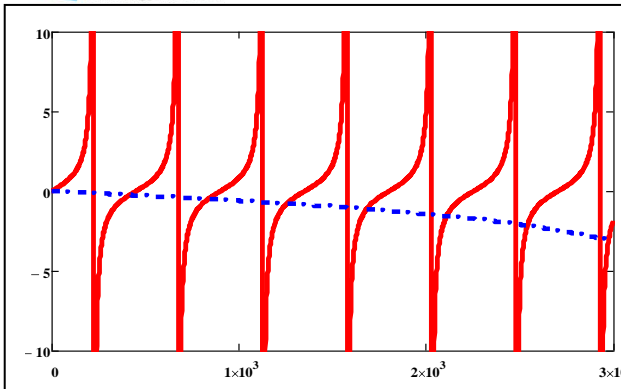


Figure 7: Graphical resolution of the transcendental equation for the both side illumination

The analysis of these curves shows a modification of eigenvalues from one side to another for a same energy irradiation value $\phi = 200$ mev. this suggests different effects of radiation and damage coefficient on the carrier density and this for different modes of illumination.

4. DENSITY OF MINORITY CARRIER IN TRANSIENT RESPONSE:

We present on figure 8, 9 and 10 the transient decay of minority carrier density for different modes of illumination and also the series expansion of equation (6) limited to one, two, and three terms. We present the front illumination, the back-side illumination and simultaneous illumination of both front and back-side.

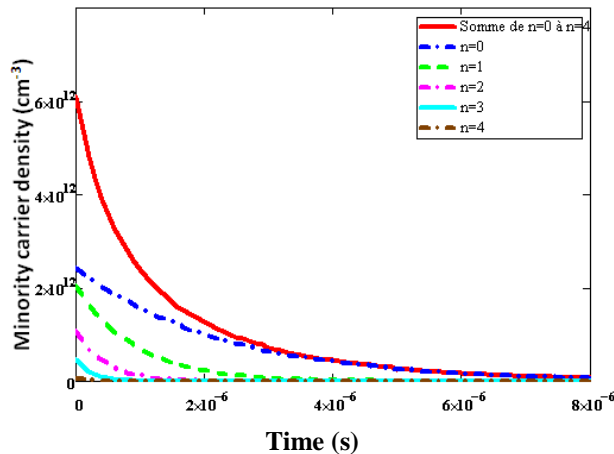


Figure 8: Transient decay versus time for front illumination

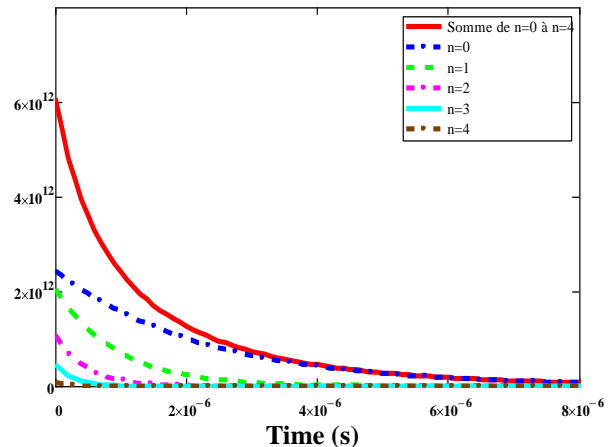


Figure 9: Transient decay versus time for back illumination

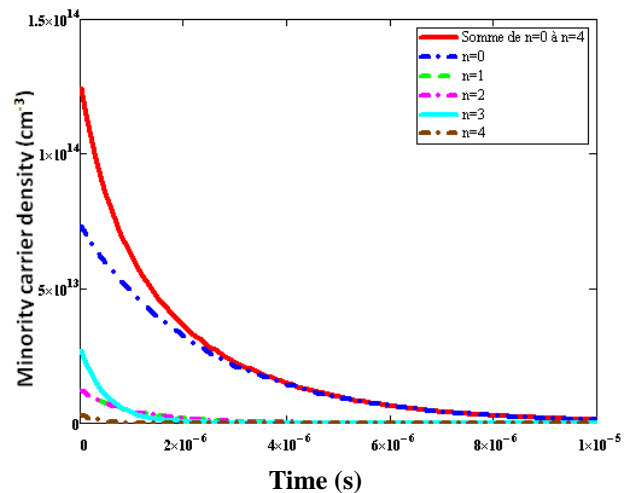


Figure 10: Transient decay versus time for both side illumination

We can see in Figure 8, 9 and 10 that, as for the front, the minority carrier densities corresponding to different values of n decrease and load all tend to the same limit for a relatively long observation time. They are all converging. The density of the fundamental mode is dominant and is joined by those harmonics which still form a block and become negligible compared with that of the fundamental mode.

However we note that the carrier density of total minority charge coincides with that of the fundamental mode from a time t_0 we can note.

This **Figure 10** also shows that the carrier density decreases with time. After time $t_0 (> 1\mu s)$, the densities of modes other than the fundamental mode becomes negligible in $\delta_{ar,0}(0, t)$.

5. EFFECT OF IRRADIATION AND DAMAGE COEFFICIENT ON MINORITY CARRIER DENSITY

We present in **figure 11** the excess minority carriers density versus irradiation energy for various damage coefficients.

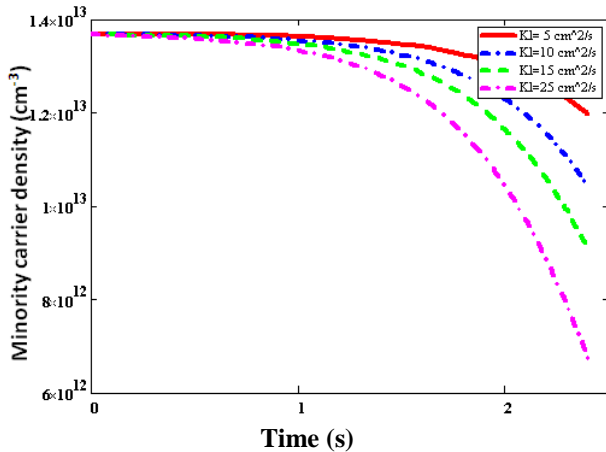


Figure 11: Carrier density versus irradiation energy Φ for various damage coefficients

We can observe that the density of minority carriers decreases with the irradiation for a damage coefficient. And it's more perceptible for higher irradiation energy and higher damage coefficient.

The excess minority carrier's density versus time is presented on figures for various irradiation energies and various damage coefficients and for the front illumination, the back-side illumination and simultaneous illumination of both front and back-side.

First, on figure 12 and 13 we present the excess minority carrier's density for front illumination.

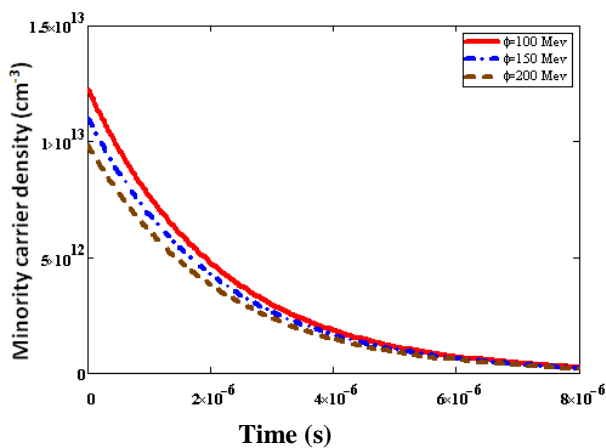


Figure 12: Variation of the carrier density versus time for different values of irradiation energy Φ

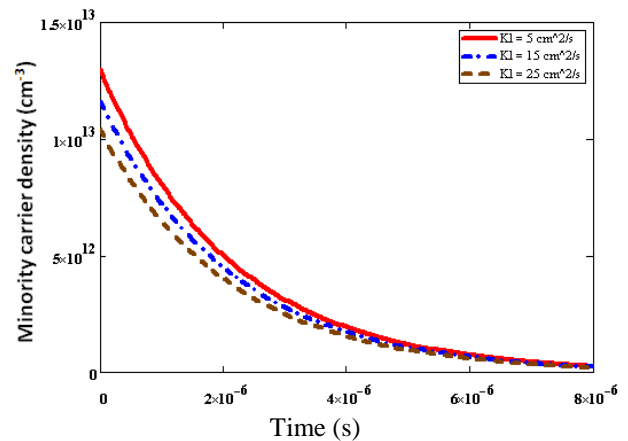


Figure 13: Variation of the carrier density versus time for different values of damage coefficient KI ,

On figure 14 and 15, the excess minority carrier's density for back illumination is presented.

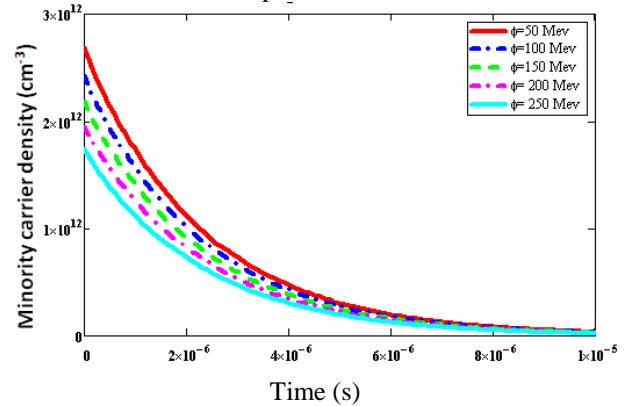


Figure 14: Variation of the carrier density versus time for different values of irradiation energy Φ

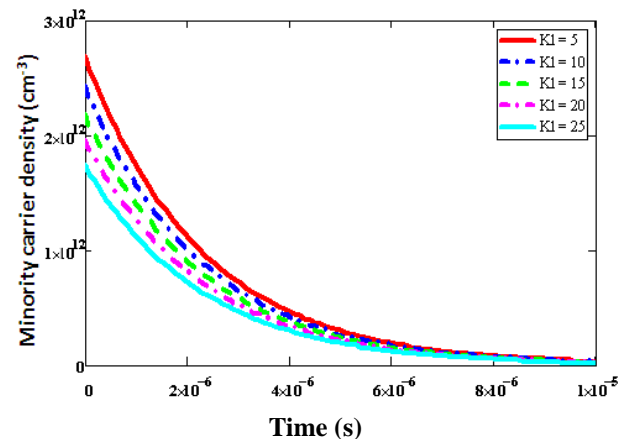


Figure 15: Variation of the carrier density versus time for different values damage coefficient KI

On figure 16 and 17, we present the excess minority carrier's density for both side illuminations.

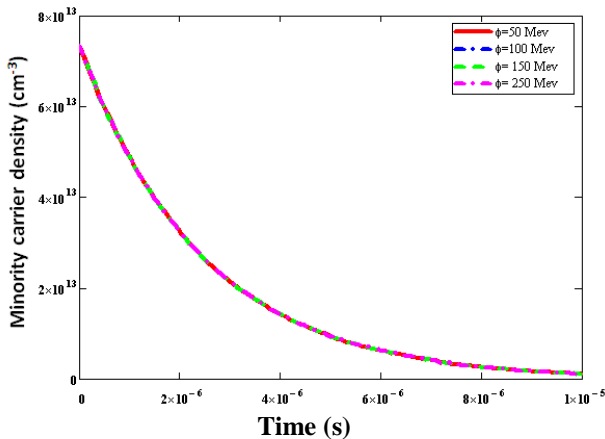


Figure 16: Variation of the carrier density versus time for different values of irradiation energy Φ

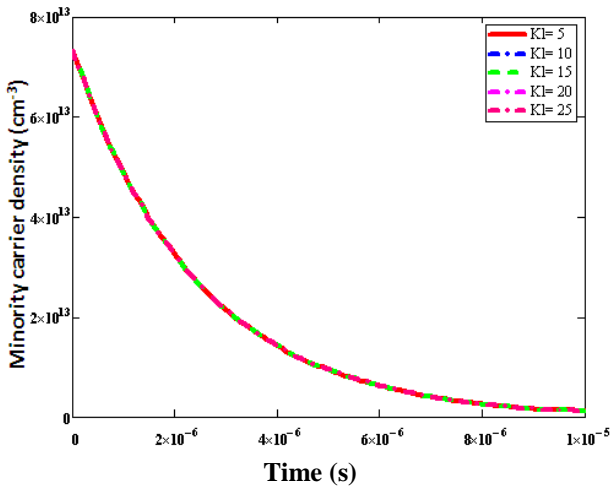


Figure 17: Variation of the carrier density versus time for different values of irradiation energy Φ

We note in **Figures 12, 13, 14 and 15** that the particle irradiation energy affects the transient variation of the carrier density. When the irradiation energy increases, the carrier density decreases, and the variation in time is faster. Thus, for a given value of the energy of radiation, we feel the same effects with the increase in the coefficient of damage. The passage of a charged particle, including an ion through the material generates a region damaged along its path, irradiation creates defects inherent in interactions between charged particles and electrons of silicon. The charged particles lose their energy in the material and the electron density decreases. **[10, 11].**

For **Figures 16 and 17** shows that the carrier density is maximum at the junction at $t = 0$ and decreases with time simultaneous illumination. The amplitude of the density remains constant when the irradiation energy increases, and we have the same behavior with increasing coefficient of damage. Illuminates when the solar cell by both sides (simultaneous illumination), the degradation caused by irradiation is quickly compensated so that you

do not feel the effect of irradiation on the carrier density. Both effects are in competition:

- Interaction particle material that tends to reduce the carrier density created;
- Permanent generation of electron-hole pair in multispectral illumination.

6. CONCLUSION

This study based on a silicon solar cell irradiated by energetic particles shows that the diffusion length depend strongly on the irradiation energy but also on the damage coefficient of these particles. The study also showed that the minority carrier's density is influenced by both the irradiation energy and the damage coefficient for front, back and simultaneous illumination. We can also extend this study to the influence of irradiation on transient photovoltage, transient photocurrent and transient capacitance for a bifacial silicon solar cell.

REFERENCES

- [1] Helmuth Spieler Introduction to Radiation-Resistant semiconductor devices and circuits. *Ernest Orlando Lawrence Berkeley National Laboratory, Physics Division*
- [2] R. J. Walters and G. P. Summers Space Radiation Effects in Advanced Solar Cell Materials and Devices Mat. Res. Soc. Symp. Proc. Vol. 692
- [3] G. SISSOKO, E. NANEMA, A. CORREA, P. M. BITEYE, M. ADJ, A. L. NDIAYE. Silicon Solar cell recombination parameters determination using the illuminated I-V characteristic. World Renewable Energy Congress, pp.1848-1851, 1998.
- [4] G. SISSOKO, C. MUSERUKA, A. CORRÉA, I. GAYE, A. L. NDIAYE. Light spectral effect on recombination parameters of silicon solar cell World Renewable Energy Congress, part III, pp.1487-1490, 1996
- [5] M.A. Ould El Moujtaba, M. Ndiaye, A.Diao, M.Thiame, I.F. Barro and G. Sissoko. Theoretical Study of the Influence of Irradiation on a Silicon Solar Cell under Multispectral Illumination. *Research Journal of Applied Sciences, Engineering and Technology* ISSN
- [6] R. K. Ahrenkiel, D. J. Dunlavy, H. C. Hamaker, R. T. Green, C. R. Lewis, R. E. Hayes, H. Fardi Time-of-flight studies of minority-carrier diffusion in $Al_xGa_{1-x}As$ homojunctions *J. Appl. Phys.* 49(12) 1986.
- [7] Mara Bruzzi Radiation Damage in Silicon Detectors for High-Energy Physics Experiments *IEEE transactions on nuclear science*, vol. 48, no. 4, august 2001.
- [8] A. RICAUD Photopiles solaires. Presses polytechniques et universitaires romandes, 1997.
- [9] Radu D. Rugescu Silicon solar cells: recombination and electrical parameters. ISBN

978-953-307-052-0, pp. 432, February 2010,
INTECH,

- [10] H. MATHIEU, H. FANET. Physique des semiconducteurs et des composants électroniques 6^{ème} Ed, Dunod, 2009
- [11] L. Andricek, D. Hauff, J. Kemmer, P. LuKewille, G. Lutz, H.G. Moser, R.H. Richter, T. Rohe, K. Stolze, A. Viehl. Radiation hard strip detectors for large-scale silicon trackers *Nuclear Instruments and Methods in Physics Research A 436 (1999)* 262-271.
- [12] I. Gaye, R. Sam, A.D. Seré, I.F. Barro, M.A. Ould El Moujtaba, R Mané, G Sissoko. Effect of irradiation on the transient response of a silicon solar cell *International Journal of Emerging Trends & Technology in Computer Science (IJETTCS)* Volume 1, Issue 3, September – October 2012 210-214.
- [13] F. I. Barro, A. Seidou Maiga, A. Wereme, G. Sissoko Determination of recombination parameters in the base of a bifacial silicon solar cell under constant multispectral light *Phys. Chem. News 56 (2010) 76-84*